Published OnlineFirst on October 12, 2010 as 10.1158/0008-5472.CAN-10-1418

Therapeutics, Targets, and Chemical Biology

Cancer Research

Prostate Cancer Radiosensitization through Poly(ADP-Ribose) Polymerase-1 Hyperactivation

Ying Dong[1,2], Erik A. Bey[1,2], Long-Shan Li[1,2], Wareef Kabbani[3], Jingsheng Yan[4], Xian-Jin Xie[4], Jer-Tsong Hsieh[5], Jinming Gao[1], and David A. Boothman[1,2]

Abstract

The clinical experimental agent, β-lapachone (β-lap; Arq 501), can act as a potent radiosensitizer *in vitro* through an unknown mechanism. In this study, we analyzed the mechanism to determine whether β-lap may warrant clinical evaluation as a radiosensitizer. β-Lap killed prostate cancer cells by NAD(P)H:quinone oxidoreductase 1 (NQO1) metabolic bioactivation, triggering a massive induction of reactive oxygen species, irreversible DNA single-strand breaks (SSB), poly(ADP-ribose) polymerase-1 (PARP-1) hyperactivation, NAD^+/ATP depletion, and μ-calpain–induced programmed necrosis. In combination with ionizing radiation (IR), β-lap radiosensitized $NQO1^+$ prostate cancer cells under conditions where nontoxic doses of either agent alone achieved threshold levels of SSBs required for hyperactivation of PARP-1. Combination therapy significantly elevated SSB level, γ-H2AX foci formation, and poly(ADP-ribosylation) of PARP-1, which were associated with ATP loss and induction of μ-calpain–induced programmed cell death. Radiosensitization by β-lap was blocked by the NQO1 inhibitor dicoumarol or the PARP-1 inhibitor DPQ. In a mouse xenograft model of prostate cancer, β-lap synergized with IR to promote antitumor efficacy. NQO1 levels were elevated in ~60% of human prostate tumors evaluated relative to adjacent normal tissue, where β-lap might be efficacious alone or in combination with radiation. Our findings offer a rationale for the clinical utilization of β-lap (Arq 501) as a radiosensitizer in prostate cancers that overexpress NQO1, offering a potentially synergistic targeting strategy to exploit PARP-1 hyperactivation. *Cancer Res; 70(20); 8088–96. ©2010 AACR.*

Introduction

Prostate cancer is the most common noncutaneous cancer in men in the United States. It occurs with the highest incidence (25%) of all cancers and is the second leading cause of cancer-related death in men (1). Radiation therapy [X-ray therapy (XRT)] using fractionated low doses of ionizing radiation (IR) is the most heavily used therapeutic method for treating primary prostate cancers. However, traditional external beam fractionated XRT using total IR doses of <68 Gy have only limited curative potential for locally advanced stages of prostate cancer, with a high (~70%) 5-year relapse rate (2). These lower doses are not efficacious for treating prostate cancer due to intrinsic radioresistance (3, 4), whereas accumulated high doses of IR cause severe side effects, such as urinary and bowel dysfunction, erectile dysfunction, and infertility. These complications are caused by damage to surrounding normal tissue by surgery, XRT, and/or chemotherapies as a result of the lack of tumor selectivity. Efficacious and tumor-selective synergistic strategies for treating human prostate cancers are in great demand.

β-Lapachone (β-lap; 3,4-dihydro-2,2-dimethyl-2*H*-naphtho[1,2-*b*]pyran-5,6-dione; also known as Arq 501), a novel antitumor quinone, has shown promise alone as a tumor-selective chemotherapeutic agent in cancers that overexpress endogenous NAD(P)H:quinone oxidoreductase-1 (NQO1; E.C. 1.6.99.2), a two-electron oxidoreductase. We previously showed that NQO1 metabolized β-lap through a futile cycle, with the parent quinone converted to a highly unstable hydroquinone form, utilizing dramatic levels of NAD(P)H. As a result, high levels of reactive oxygen species (ROS) are created, causing DNA lesions in $NQO1^+$ cells (5–7). At LD_{90} and higher doses of β-lap (≥4 μmol/L), poly(ADP-ribose) polymerase-1 (PARP-1), a DNA damage sensor, is hyperactivated and extensive NAD^+/ATP depletion ensues. PARP-1 hyperactivation required rapid Ca^{2+} release from endoplasmic reticulum stores, a result of ROS formation (8). Subsequently, loss of NAD^+/ATP results in influx of Ca^{2+}, leading to the activation and nuclear translocation of μ-calpain. Activation of μ-calpain causes a unique caspase-independent programmed necrotic cell death (8, 9). Importantly, β-lap killing of cancer cells is NQO1 specific and independent of cell cycle status, caspase activities, and

Authors' Affiliations: Departments of [1]Pharmacology, [2]Radiation Oncology, [3]Pathology, [4]Biostatistics and Clinical Sciences, and [5]Urology, Simmons Comprehensive Cancer Center, University of Texas Southwestern Medical Center, Dallas, Texas

Note: Supplementary data for this article are available at Cancer Research Online (http://cancerres.aacrjournals.org/).

Y. Dong and E.A. Bey contributed equally to this work.

Corresponding Author: David A. Boothman, Laboratory of Molecular Stress Responses, Program in Cell Stress and Cancer Nanomedicine, 6001 Forrest Park, ND2.210K, Mailstop 8807, Dallas, TX 75390-8807. Phone: 214-645-6371; Fax: 214-645-6347; E-mail: David.Boothman@UTSouthwestern.edu.

doi: 10.1158/0008-5472.CAN-10-1418

Rb or p53 status (6, 7, 10–12). Because NQO1 is highly expressed in many human cancers, including prostate, lung, pancreatic, and breast cancers, β-lap has become an attractive agent for tumor-selective cancer chemotherapy.

PARP-1 is an abundant nuclear enzyme essential for repair of DNA single-strand breaks (SSB) and an important damage sensor, for which numerous groups are developing inhibitors (13–15), particularly after its identification as a synthetic lethal target in BRCA1/2 breast cancers (16, 17). PARP-1 is essential for base excision repair (BER), SSB, and possibly other DNA repair processes (18, 19). PARP-1 is activated after binding DNA strand breaks and uses NAD^+ as a substrate to form long branched polymers of poly(ADP-ribose) (PAR). PARP-1–mediated poly(ADP-ribosylation) recruits various nuclear acceptor proteins, such as XRCC1, histones, and PARP-1 itself, to assemble other repair complexes to execute DNA repair [i.e., BER, SSB, and double-strand break (DSB) repair]. However, in response to excessive DNA damage, PARP-1 can be hyperactivated, converting its DNA repair capacity to initiation of programmed necrosis, due to dramatic NAD^+ and ATP depletions. PARP-1 hyperactivation and programmed necrosis have been documented in several cellular responses, including ischemia-reperfusion, myocardial infarction, and severe ROS-induced injury (20). To date, however, the only cytotoxic agent able to harness this cell death pathway in a tumor-selective manner and at clinically relevant doses is β-lap (6, 21).

We previously showed that β-lap was an efficient radiosensitizer of specific cancer cells when given immediately after or during IR *in vitro* (22, 23). However, these studies stalled due to a lack of knowledge about the mechanism of action of the agent and an inability to efficaciously deliver the drug. Based on our recent elucidation of the mechanism of action of β-lap as a single agent (8, 9), we hypothesized that PARP-1 hyperactivation was a key factor mediating synergy between sublethal doses of IR and β-lap. Here, we show for the first time that PARP-1 hyperactivation is the principal determinant governing β-lap–radiosensitizing effects in $NQO1^+$ human prostate cancer cells, causing early and rapid PAR-modified PARP-1 accumulation and synergistic ATP loss after IR + β-lap treatments. Along with dicoumarol (a specific inhibitor of NQO1), DPQ (a specific PARP-1 inhibitor) blocked dramatic ATP depletion and apoptosis, confirming an essential role of NQO1-dependent PARP-1 hyperactivation in mediating synergy between these two agents. Antitumor studies using PC-3 xenografts that have endogenously elevated NQO1 levels in athymic mice showed significantly enhanced antitumor efficacy using various combined sublethal doses of β-lap + IR. Thus, β-lap treatment in combination with XRT represents the first effective tumor-selective therapy that exploits PARP-1 hyperactivation for the treatment of cancers that have elevated NQO1 levels.

Materials and Methods

Chemicals and reagents

β-Lap, synthesized by Dr. Bill Bornmann (M.D. Anderson, Houston, TX), was dissolved in DMSO at 47 mmol/L, and concentrations were verified by spectrophotometry. Hoechst 33258, hydrogen peroxide (H_2O_2), staurosporine, cytochrome *c*, etoposide, DPQ (3,4-dihydro-5[4-(1-piperindinyl)butoxy]-1(2*H*)-isoquinoline), and dicoumarol (24) were purchased from Sigma-Aldrich.

Cell culture

PC-3, DU145, and LNCaP human prostate cancer cells were originally obtained from Dr. George Wilding (University of Wisconsin-Madison). PC-3 and DU145 cells were grown in RPMI 1640 (Invitrogen) with 5% fetal bovine serum (FBS) and LNCaP cells were grown in DMEM (Invitrogen) with 10% FBS. Cells were cultured at 37°C in a 5% CO_2-95% air humidified atmosphere and were free of *Mycoplasma*.

Western immunoblotting

Whole-cell extracts were prepared, proteins were separated by SDS-PAGE, and Western blots were developed using SuperSignal West Pico Chemiluminescent substrate (Thermo Scientific) and exposed using autoradiography film (Denville Scientific, Inc.). An antihuman NQO1 antibody was kindly provided to us by Dr. David Ross (University of Colorado Health Science Center, Denver, CO) and used at 1:5,000 dilution overnight at 4°C. Both PAR (BD Pharmingen) and γH_2AX (Upstate) antibodies were used at 1:2,000 and 1:1,000 dilutions, respectively. β-Actin or α-tubulin levels were used as loading controls.

Relative survival assays

Relative survival was assessed by DNA content and colony forming assays as described (25). Briefly, for DNA content, cells were seeded at 5×10^3 per well in 48-well plates and allowed to attach overnight. Cells were then mock treated or treated with various doses of β-lap (for 2 hours) in the presence or absence of dicoumarol as indicated. Drug-free medium was then added and cells were allowed to grow for 5 to 7 days until control cells reached ~100% confluence. DNA content was then determined by Hoechst 33258 staining and fluorescence detection using a plate reader (Perkin-Elmer; ref. 21). Relative survival assays after combined treatment were confirmed by colony-forming ability assays (25). Results were reported as mean ± SE from at least three independent experiments.

Total and oxidized glutathione assays

Disulfide and total glutathione (GSH and GSSG, respectively) levels were determined using a spectrophotometric recycling assay (26). After treatments, whole-cell homogenates were prepared (11). Data were expressed as %GSSG/total, normalized to protein content, following the procedure of Lowry and colleagues (27). Data were shown as mean ± SE of experiments performed at least three times.

Alkaline and neutral comet assays

DNA lesions, including total base damage, DSBs, and SSBs, versus DSBs were assessed using single-cell gel electrophoretic comet assays under alkaline or neutral conditions, respectively (Trevigen). Slides were stained with SYBR Green and visualized using a Nikon Eclipse TE2000-E fluorescence

microscope. Digital photomicrographs were taken and comet tail lengths quantified using NIH Image J software. Each data point represented the average of 100 cells ± SE, and data were representative of experiments performed in triplicate.

Nucleotide analyses

Changes in intracellular NAD^+ levels were measured (6) and levels were expressed as percent treated divided by control (% T/C) ± SE from at least three individual experiments. ATP levels were analyzed from whole-cell extracts using CellTiter-Glo Luminescent Cell Viability Assays (Promega) following the manufacturer's instructions. Data were graphed as mean ± SE from at least three independent experiments in triplicate.

Apoptotic assays

Apoptosis was quantified using ApoDirect [terminal deoxyribonucleotidyl transferase–mediated dUTP nick end labeling (TUNEL)] assays from BD Pharmingen (21). Samples were analyzed by using a FC-500 flow cytometer (Beckman Coulter Electronics) and Elite acquisition software. Data were expressed as mean ± SE from three independent experiments.

Antitumor efficacy

Athymic *nu/nu* mice were purchased from Charles River Laboratories International, Inc. All animals were housed in a pathogen-free facility with 24-h access to food and water. Experimental protocols were approved by the institutional Animal Care and Use Committee at the University of Texas Southwestern. PC-3 cells (5×10^6) were s.c. injected into the right thighs of athymic nude mice, and tumor volumes were allowed to reach ~350 mm^3. Mice (five mice per group) were then randomly grouped with no statistical differences in tumor sizes among the six groups. Mice were then mock treated or exposed to various IR doses followed immediately by treatment with various doses (10–30 mg/kg) of β-lap-HPβ-CD or HPβ-CD. When used, various doses of IR were given locally first to tumor sites with whole-body shielding. Mice were exposed to one treatment regimen, consisting of mock or XRT, immediately followed by HPβ-CD alone or various β-lap-HPβ-CD doses administered via tail vein injections for five IR + β-lap exposures. Tumor volumes were measured by caliper (length × width × width/2) every other day. Mice were sacrificed when tumors reached 2 cm^3 or 10% total body weight.

Statistical analyses

For relative survival, different IR + β-lap combinations were fit with simple multitarget models in SigmaPlot for Windows version 11.0. For synergy, a statistical definition of synergy (28) was used and calculations were performed by fitting experimental data with the Machado and Robinson model using the R code (29). The equitoxic doses listed in Table 1 were calculated using the parameters of the model of Machado and Robinson obtained in fitting. Regression analyses of tumor growth profiles *in vivo* in six tested groups were analyzed using a mixed model approach with AR (1) correlation structures. Log-rank tests were applied to survival analyses (Kaplan-Meier curves). In general, P values of ≤0.05 using two-sided Student's t test were considered significant. All statistical analyses were performed using SAS 9.1 Service Pack 4.

Results

β-Lap induces prostate cancer cell death through NQO1-induced ROS formation and SSBs

Our immunohistochemical analyses of human prostate tumor and associated normal tissue revealed that ~60% of these cancers had elevated NQO1 levels (Supplementary Fig. S1). Using human PC-3 prostate cancer cells that express high levels of endogenous NQO1, we showed that the cytotoxic effects of β-lap were NQO1 dependent (inhibited by dicoumarol Fig. 1A). This was confirmed in DU145 and in NQO1-proficient ($NQO1^+$) versus NQO1-deficient ($NQO1^-$) LNCaP cells (Supplementary Fig. S2). Importantly, only ~120 minutes of exposure to 4 μmol/L β-lap was sufficient to achieve maximal cytotoxicity (Fig. 1A), where significant levels of glutathione were oxidized (note rapid and elevated levels of %GSSG in 20–30 minutes; Fig. 1B), suggesting dramatic ROS formation. Dramatic increases in SSBs were seen by alkaline comet assays, but DSBs, as assessed by neutral comet assays, were not noted (Fig. 1C and D). Similar results were found using DU145 and $NQO1^+$ LNCaP cells (Supplementary Fig. S2). In contrast, $NQO1^-$ LNCaP cells were not responsive to β-lap as described (5).

The DNA damage and repair responses of β-lap–treated NQO1-expressing PC-3 cells were compared with their responses after IR treatment (Fig. 1E and F). Extensive DNA lesions were noted in PC-3 cells after exposure to 4 μmol/L β-lap, equivalent to 20 Gy by alkaline assays. However, neutral comet assays revealed DSBs after IR, but not after β-lap, exposure (not shown). Exposure of PC-3 cells to IR (20 Gy)

Table 1. Equitoxic doses comparing single to combined treatment in PC-3 cells

IR (Gy)	β-Lap (μmol/L)	Equivalent dose of IR (Gy)	Equivalent dose of β-lap (μmol/L)
0	1	0.6	1
0	2	0.9	2
0	3	1.2	3
1	1	1.5	4.1
1	2	1.9	5.5
1	3	2.3	6.9
2	1	2.5	7.9
2	2	2.9	9.6
2	3	3.2	11.2
3	1	3.5	12.5
3	2	3.9	14.2
3	3	4.2	16

NOTE: Values of equivalent doses were calculated using parameters obtained from fitting the data from three independent experiments done in triplicate with Machado's model.

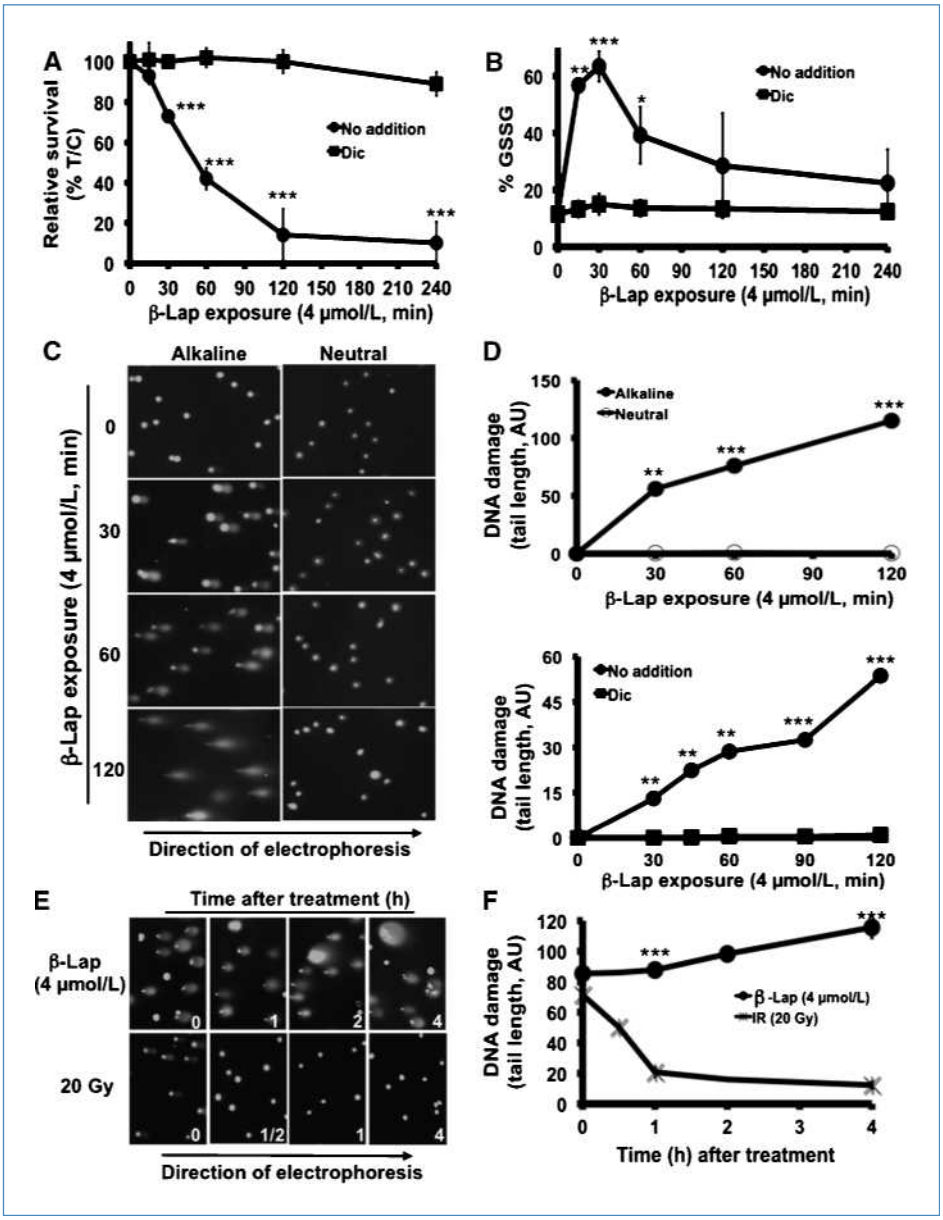

Figure 1. β-Lap–induced, NQO1-mediated ROS formation and SSBs are required for cell death in human prostate cancer cells. A, relative survival of PC-3 cells after β-lap treatment in the presence or absence of dicoumarol (Dic; 40 μmol/L). Points, mean of three independent experiments performed in sextuplicate; bars, SE. B, ROS formation was indirectly monitored using the oxidized glutathione (GSSG) recycling assay in β-lap–exposed PC-3 cells in the presence or absence of 40 μmol/L dicoumarol. Points, mean; bars, SE. Representative of three experiments performed in duplicate. C, alkaline versus neutral comet assays to assess total DNA damage or DSBs, respectively. H_2O_2 and etoposide were used as positive controls for agents causing mostly SSBs or DSBs, respectively (not shown). D, DNA damage assessment [arbitrary units (AU) of comet tail lengths] using NIH Image J software. Top graph as indicated; bottom graph, alkaline conditions. Points, mean from 100 cells; bars, SE. E, DNA damage in PC-3 cells after IR (20 Gy) versus β-lap (4 μmol/L, 2 h). F, comet tail lengths (arbitrary units) assessed using NIH Image J software. Points, mean from 100 cells; bars, SE. ***, $P < 0.001$; **, $P < 0.01$; *, $P < 0.05$ (*t* test).

resulted in DNA damage that was quickly repaired within 1 hour after treatment, whereas DNA damage created by 4 μmol/L β-lap was not repaired, but escalated over the 4-hour time period assessed, suggesting repair inhibition.

PARP-1 hyperactivation mediates β-lap–induced programmed cell death

Exposure of PC-3 cells to lethal doses of β-lap (Fig. 2A) caused extensive PARP-1 hyperactivation, with significant PAR accumulation within 10 to 20 minutes that was blocked by dicoumarol (Fig. 2B). Loss of PAR formation in β-lap–treated PC-3 cells, which was noted from 40 to 60 minutes, was most likely due to NAD^+ substrate depletion (Fig. 2C), as well as functional PAR glycohydrolase (30). PARP-1 hyperactivation was accompanied by dramatic NAD^+ and ATP losses as a function of (*a*) time (Fig. 2C), where metabolite levels were exhausted within 120 minutes of β-lap exposure, and (*b*) dose, where loss of ATP corresponded well with cytotoxicity (Fig. 2A and D). Loss of intracellular nucleotide levels (NAD^+/ATP) and lethality of β-lap–treated PC-3 cells were blocked by dicoumarol (40 μmol/L). Dicoumarol also prevented PARP-1 hyperactivation, NAD^+ and ATP losses, and cytotoxicity in DU145 cells after β-lap exposure (Supplementary Fig. S3).

Synergy between IR and β-lap is mediated by DNA damage, reaching a threshold for PARP-1 hyperactivation

We previously reported that the combination of IR and β-lap synergistically killed specific cancer cells (31); however,

the mechanism of synergy was not elucidated. PC-3 cells were treated with single doses of IR (1–3 Gy) followed by exposure to low, nontoxic doses of β-lap (1–3 μmol/L). Synergy was noted with all IR and β-lap combinations tested (Fig. 3A), corresponding to synergistic increases of PAR levels after combined treatments, but not after single agent exposures. For example, dramatic PAR formation in PC-3 cells treated with 1 Gy + 3 μmol/L β-lap was noted at 60 minutes, with no apparent PAR levels in cells after each agent alone (Fig. 3B). Similar responses were noted in NQO1$^+$ LNCaP and DU145 cells, but not in genetically matched NQO1$^-$ LNCaP cells (Supplementary Figs. S4A and S5B, respectively). Synergy was prevented by dicoumarol in NQO1$^+$ prostate cancer cells, corresponding to the formation of DNA lesions (noted by alkaline comet and γH2AX foci formation) that presumably reached threshold levels required for PARP-1 hyperactivation (Supplementary Fig. S5). Synergy between IR and β-lap in PC-3 cells was accompanied by dramatic losses of ATP (Fig. 3C and D, synergy between 2 or 3 Gy and 3 μmol/L β-lap) and NAD$^+$ (not shown). Importantly, synergistic losses of ATP in PC-3 cells following 2 or 3 Gy + 3 μmol/L β-lap were prevented by pre- and co-treating the cells with DPQ, a specific PARP-1 inhibitor (Fig. 3C and D, respectively) that prevented cell death induced by β-lap alone in various endogenously overexpressing NQO1 cancer cells (6, 21). Synergistic ATP loss was also observed in NQO1$^+$ LNCaP cells (Supplementary Fig. S4B).

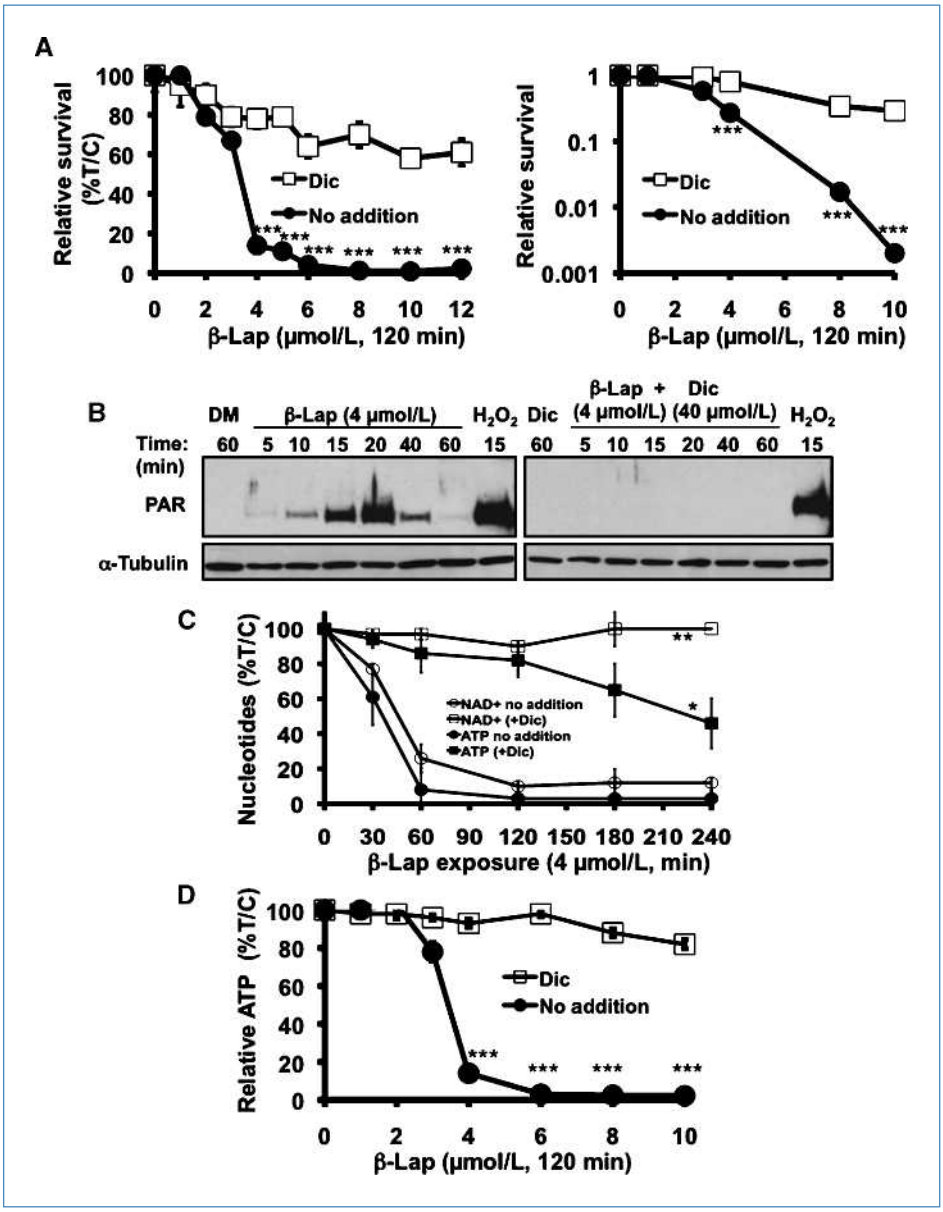

Figure 2. NQO1-dependent cytotoxicity correlates with PARP-1 hyperactivation, nucleotide depletion, and PAR formation in prostate cancer cells exposed to β-lap. A, relative survival (left, DNA content; right, colony formation) of PC-3 cells exposed for 120 min to varying doses of β-lap in the presence or absence of dicoumarol (40 μmol/L). Points, mean of three independent experiments; bars, SE. B, Western blot analyses of PAR formation in PC-3 cells treated with DMSO (DM) or 4 μmol/L β-lap in the presence or absence of dicoumarol at the indicated times. C, PC-3 cells were treated as described in B, and cells harvested at the indicated times were analyzed for NAD$^+$ and ATP levels. Points, mean of experiments performed three times in triplicate; bars, SE. D, ATP in β-lap–exposed PC-3 cells treated with various β-lap doses in the presence or absence of dicoumarol (40 μmol/L). Points, mean of six replicates from three independent experiments; bars, SE. ***, $P < 0.001$; **, $P < 0.01$; *, $P < 0.05$ (*t* tests).

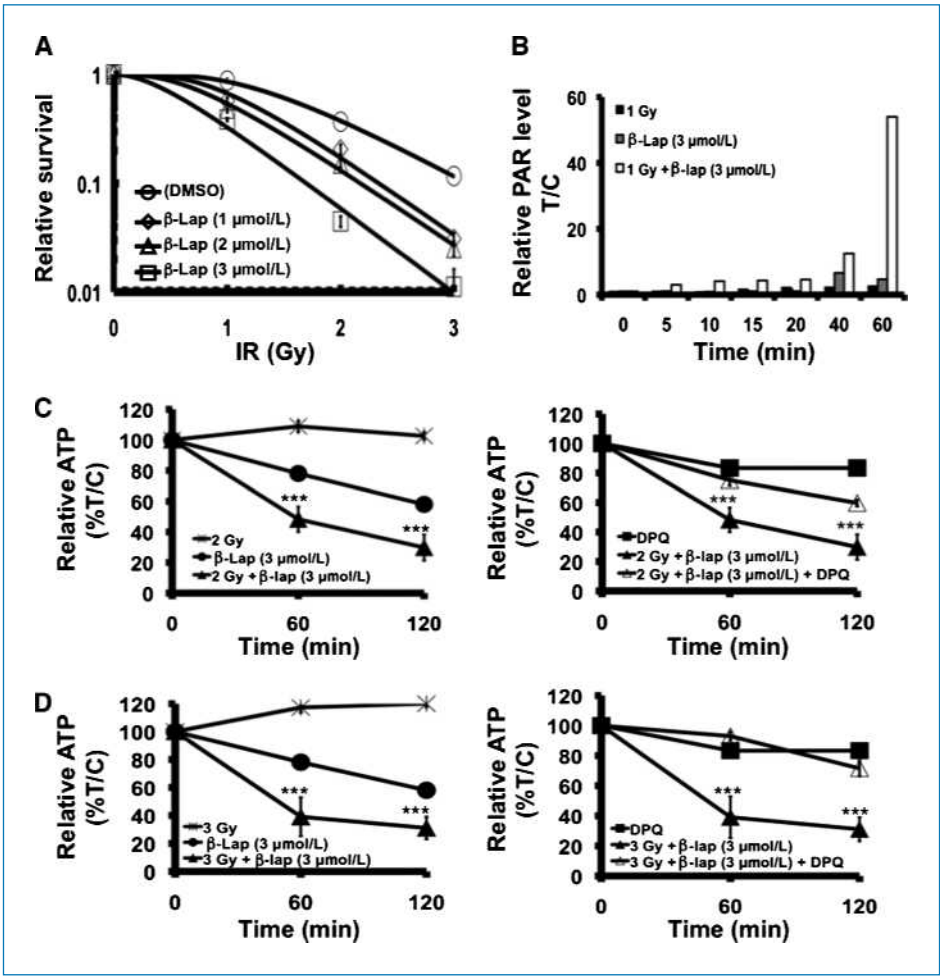

Figure 3. Synergy between IR and β-lap is mediated by PARP-1 hyperactivation. A, β-Lap exposure sensitizes PC-3 cells to IR. Points, mean of three independent experiments repeated in triplicate; bars, SE. $0 < \eta < 1$ (Machado's model). B, quantified PAR formation in PC-3 cells after various treatments. T/C, x-fold change. C and D, synergistic ATP loss observed after IR + β-lap combinations (left). DPQ, a specific PARP-1 inhibitor, blocked the synergistic ATP depletion effects of IR + β-lap (right). Points, mean of experiments performed three times in octuplets. ***, $P < 0.001$, comparing each data point to those of single treatments (*t* test).

Synergy between IR and β-lap exposures involves atypical PARP-1 cleavage and TUNEL$^+$ programmed necrosis

Loss of survival as a result of β-lap treatment correlated well with TUNEL$^+$ apoptotic responses (32). The synergistic cytotoxic responses of NQO1$^+$ PC-3 cells after IR + β-lap treatment were confirmed by analyzing apoptosis (Fig. 4A). Treatment of PC-3 cells with 1 to 3 Gy, each in combination with 2 μmol/L β-lap, resulted in significant increases in apoptotic cells within 72 hours (Fig. 4A), corresponding directly to loss of colony forming ability (Fig. 3A). Indeed, all combination therapies of IR with β-lap (Table 1) reveal synergy at these low doses of each agent. For example, treatment of PC-3 cells with nonlethal agents (alone) in combination with IR (i.e., 1 Gy + 1 μmol/L β-lap) was the same as treating cells with a lethal dose of 4 μmol/L β-lap. Similar responses were noted in NQO1$^+$ LNCaP cells, in which synergistic levels of apoptosis and atypical PARP-1 cleavage at 72 hours after treatment were noted (Supplementary Fig. S6). Synergy between IR and β-lap was prevented by DPQ (Fig. 4A) or dicoumarol, and was not observed in NQO1$^-$ LNCaP cells. In contrast, different low doses of IR alone (i.e., 1–3 Gy) only led to 2 ± 2%, 5 ± 3%, and 9 ± 3% apoptosis, respectively. Similarly, a low sublethal dose of 2 μmol/L β-lap in NQO1$^+$ PC-3 cells resulted in minimal apoptosis (i.e., 5 ± 2%; Fig. 4A).

Cell death caused by a lethal dose of β-lap in prostate cancer cells with endogenous elevation of NQO1 involves activation of μ-calpain and atypical cleavage of PARP-1 (9), as noted after 4 μmol/L β-lap treatment (Fig. 4B, lane 7). Similarly, exposure of PC-3 cells to IR + β-lap involved synergistic apoptotic responses, above the additive levels with IR or β-lap alone. Atypical PARP-1 cleavage (i.e., formation of an ~60 kDa PARP-1 fragment) in combination-treated cells was noted (Fig. 4B), resulting from activation and nuclear translocation of μ-calpain (9). Similar atypical PARP-1 cleavage events accompanied IR + β-lap synergy in NQO1$^+$ LNCaP cells (Supplementary Fig. S6B).

Efficacy *in vivo* of the combination of IR and β-lap

To date, the efficacy of β-lap against human prostate cancer xenografts expressing elevated levels of endogenous NQO1 has not been shown. Using the current clinical formulation of the drug (i.e., Arq 501) conjugated with HPβ-CD, we showed significant efficacy of β-lap-HPβ-CD when administered at 10 or 20 mg/kg in combination with 2-Gy fractions of IR (Fig. 5A). Mice (five per group) bearing PC-3 xenografts

with an average tumor volume of ~350 mm^3 were exposed to five doses of IR alone, β-lap-HPβ-CD alone, or IR + β-lap-HPβ-CD combinations every other day between days 1 and 9. All drug treatments were administered by i.v. injection. Treatment of mice with β-lap-HPβ-CD at 10 or 20 mg/kg exhibited neither antitumor efficacy nor morbidity or mortality. Although mice treated with 2-Gy fractions (five treatments, every other day) resulted in significant tumor growth delay (average, 26 days; Fig. 5; Supplementary Fig. S7A and Supplementary Table S1), combinations of 2-Gy IR with 10 or 20 mg/kg β-lap-HPβ-CD resulted in significant tumor regression beyond the additive levels with IR or β-lap-HPβ-CD treatments alone. Ninety percent (9 of 10) of animals exposed to IR + 10 or 20 mg/kg β-lap-HPβ-CD were "apparently cured," showing no further tumor growth for up to 150 days (Fig. 5B; Supplementary Table S1). In contrast, 90% PC-3-bearing mice treated with β-lap-HPβ-CD alone (10 or 20 mg/kg) died within 40 days, similar to control mice treated with vehicle (HPβ-CD) alone. Mice treated with IR (2 Gy) alone showed an obvious delay in tumor growth (Fig. 5A); however, all mice eventually died (sacrificed when tumor volumes were >10% of their weight). Finally, although treatment of mice with 2 Gy + 30 mg/kg β-lap-HPβ-CD resulted in statistically equivalent tumor growth delay and "apparent cures" (Supplementary Table S1), we noted that the dose was close to the maximum tolerated dose of the drug (Supplementary Fig. S7B). Collectively, we treated 15 mice (3 × 5 mice per group) with 2 Gy + 10 to 30 mg/kg β-lap-HPβ-CD, noting dramatic synergistic responses that were statistically superior ($P < 0.001$) to the 2 Gy alone or β-lap-HPβ-CD alone (10–30 mg/kg) regimen (Supplementary Table S1). Data from a representative experiment are presented in Fig. 5A.

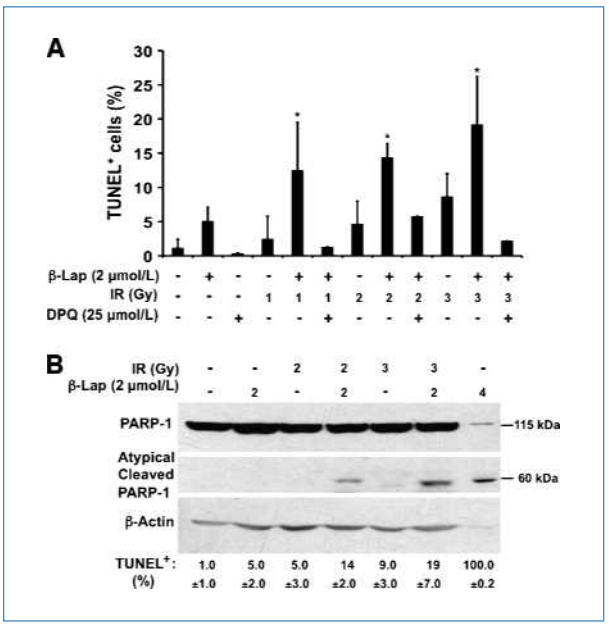

Figure 4. Combined treatment with sublethal doses of IR and β-lap promotes apoptosis and atypical PARP-1 cleavage. A, PC-3 cells were exposed to the indicated treatments for 2 h, and whole-cell extracts prepared at 72 h; apoptosis was monitored by TUNEL reactions. Columns, mean from three independent experiments; bars, SE. *, $P < 0.05$, between combined and single treatment regimens. DPQ blocked apoptosis in all combinations ($P < 0.01$). B, PC-3 cells were treated as described in A and harvested at 48 h for Western blot analyses. A lethal β-lap dose of 4 μmol/L was used as a positive control to indicate the ~60-kDa atypical cleaved PARP-1. TUNEL assay data were mean ± SE from three independent experiments.

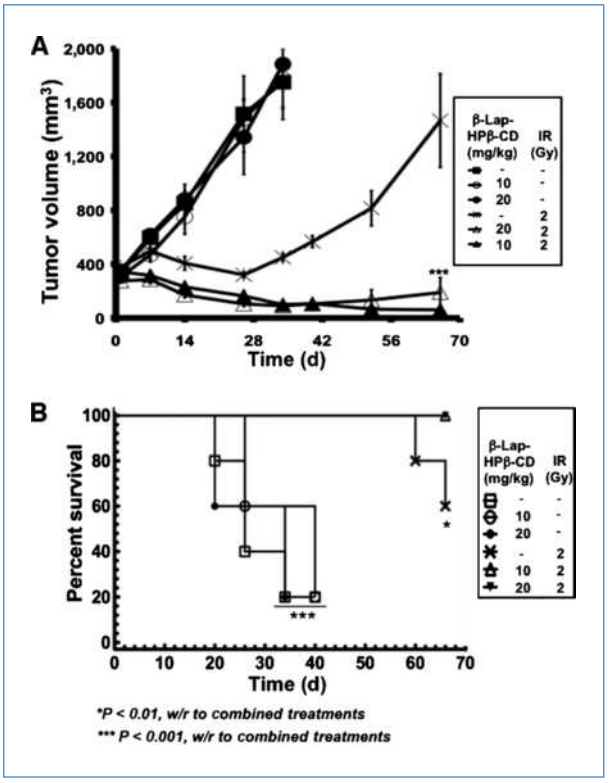

Figure 5. IR + β-lap elicits synergistic antitumor activity in PC-3 tumor xenografts. A, antitumor efficacy using different treatment regimens in athymic mice bearing PC-3 xenografts. Mice bearing 350 mm^3 PC-3 xenografts were treated once every other day starting on day 1, for five treatments (Materials and Methods). Points, mean; bars, SE. Mixed model analyses showed significant differences for combined versus single treatments, including untreated controls (***, $P < 0.0001$). B, Kaplan-Meier survival curves reflect significantly enhanced antitumor efficacy using various IR + β-lap regimens. ***, $P < 0.001$; *, $P < 0.05$, each single treatment versus combined treatment (log-rank test). Note 2 Gy + 10 or 20 mg/kg β-lap-HPβ-CD were identical.

Discussion

In general, there is a great need for improved combination therapy, where XRT is combined with tumor-selective therapies to increase antitumor efficacy, while simultaneously decreasing normal tissue toxicity. For XRT, the intrinsic radioresistance of many tumors poses significant clinical obstacles, limiting efficacy (33). Since the first stereotactic body radiotherapy (SBRT) was developed in 1991, the method has been refined to decrease high doses of IR used in local primary or focal metastatic lesions (34, 35). Recently,

hypofractionated SBRT delivered by CyberKnife using three to five fractionated high-dose XRT resulted in minimal toxicity, lowering short-term PSA and preserving normal tissue function in men with localized prostate cancer (36, 37). However, such SBRT regimens are not suited to treat metastatic disease, and long-lasting normal tissue toxicity is still problematic. Our data showed that XRT combined with β-lap post-treatments selectively killed $NQO1^+$ prostate cancer cells, offering a strategy to use lower efficacious doses of IR for targeted therapy while simultaneously eliminating prostate cancer micrometastases. This therapy should be applicable to all cancers that have elevated levels of NQO1.

β-Lap is the only agent that selectively kills tumor cells by PARP-1–mediated, μ-calpain–directed programmed necrosis at clinically relevant doses. Detailed knowledge of its mechanism of action can be exploited for improving XRT of tumors with elevated NQO1 levels. The tumor-selective nature of the therapy, for those individuals with elevated NQO1 levels, should allow reduced IR exposures while achieving improved antitumor efficacy and simultaneously avoiding normal tissue complications. Importantly, resistance to β-lap–induced, NQO1-directed antitumor cytotoxicity has not been noted to date (10, 12), most likely due to the diverse downstream effects of this drug in NQO1-containing cells, including dramatic alterations in nucleotide metabolism (i.e., NAD^+/ATP losses), DNA damage, and loss of Ca^{2+} homeostasis.

DNA damage response pathways have become new and effective targets to potentiate XRT. Considerable interest has been focused on targeting PARP-1 to eliminate DNA repair and enhance the sensitivity of cancer cells to other DNA-damaging agents, including chemotherapeutic agents and IR (38–40). None of these approaches currently exploit PARP-1 hyperactivation, which requires a "threshold" of DNA lesions to activate a suicide pathway. Our data suggest that massive levels of ROS formed by β-lap lead to persistent base lesions that are ultimately converted to SSBs by BER, which, in turn, hyperactivate PARP-1. Due to dramatic NAD^+/ATP losses, other repair processes that depend on energy are blocked, preventing repair of lethal DSBs created by IR. The delayed increase in γH2AX formation after PAR formation (Supplementary Fig. S2B) is consistent with PARP-1 break protection, followed by SSBs and eventually DSB formation detected by ATM, resulting in γH2AX foci formation.

Current phase I/II clinical trials of β-lap (i.e., Arq 501) were limited by high doses of HPβ-CD vehicle that caused hemolytic anemia, limiting efficacy. We show that nontoxic doses of β-lap-HPβ-CD can be delivered in combination with XRT for efficacious antitumor therapy of prostate cancers expressing endogenously elevated NQO1 levels. The efficacy of combination therapy was much greater than that of single regimens alone (Table 1). Synergy between IR and β-lap *in vitro* was determined using several applied models (28, 29, 41, 42), but the Machado model gave the most consistent results. Overall, the ability of β-lap to sensitize IR-exposed $NQO1^+$ tumor cells relates to the higher DNA lesions created by the drug/radiation combination that meets a threshold level required for PARP-1 hyperactivation and synergistic cell death, consistent with prior findings (31).

Here, we show that lethal doses of β-lap alone or sublethal doses of IR + β-lap kill $NQO1^+$ prostate cancer tumor cells as a result of extensive ROS formation, massive DNA damage, PARP-1 hyperactivation, and dramatic energy depletion (Figs. 1 and 2). Energy depletion, in turn, dramatically inhibits DNA repair. PAR formation was detected after combined IR + β-lap treatments, but not after single sublethal exposures of IR or β-lap alone in $NQO1^+$ LNCaP cells. LNCaP $NQO1^-$ cells were not responsive (Supplementary Fig. S4A). Downstream, dramatic metabolic changes culminated in catastrophic Ca^{2+} homeostasis. Atypical PARP-1 cleavage was noted after combination therapy, but not after sublethal IR or β-lap single treatment alone, in $NQO1^+$ human prostate cancer cells (Fig. 4B; Supplementary Fig. S6B), consistent with μ-calpain–mediated $TUNEL^+$ programmed cell death responses after lethal doses of β-lap (6, 9). Because β-lap alone or XRT + β-lap combination therapy kills cells independent of cell cycle or p53 status, it represents a controllable synergistic therapy for slow-growing $NQO1^+$ prostate cancer, as well as for non–small cell lung, pancreatic, and breast cancers, whose elevated NQO1 levels are more frequent and even greater than those of enzyme activities in associated normal tissue. Importantly, we show for the first time that XRT + β-lap-HPβ-CD caused significant long-term tumor regression with no tumor recurrence. The use of β-lap to synergize with IR (XRT) offers selectivity that can be rapidly individualized, such as for those prostate cancer patients whose NQO1 levels are elevated. Patients with easily detectable polymorphisms in NQO1 can be screened using blood-derived SNP analyses and excluded from treatment (21). Although efficacious, we theorize that improved drug delivery using millirods for brachytherapy (43) or nanoparticle micelles (44) with XRT will further augment antitumor efficacy for the treatment of cancers with elevated NQO1 levels, such as for prostate cancer.

Disclosure of Potential Conflicts of Interest

No potential conflicts of interest were disclosed.

Acknowledgments

We thank the Tissue Procurement and Biostatistics Shared Resources, supported by the Harold C. Simmons Comprehensive Cancer Center at UT Southwestern Medical Center. This is CSCN #052 from the Cell Stress and Cancer Nanomedicine (CSCN) program. We are also grateful for support from the Robert and Virginia Payne endowment to D.A. Boothman. This work is dedicated to Ray Boothman (1928-2010).

Grant Support

National Cancer Institute/NIH grant 2 R01 CA102792-08, DoD grant W81XWH-06-1-0198 (D.A. Boothman), and DoD postdoctoral grant W81XWH-08-1-0 (Y. Dong).

The costs of publication of this article were defrayed in part by the payment of page charges. This article must therefore be hereby marked *advertisement* in accordance with 18 U.S.C. Section 1734 solely to indicate this fact.

Received 04/20/2010; revised 07/19/2010; accepted 08/08/2010; published OnlineFirst 10/12/2010.

References

1. Jemal A, Siegel R, Ward E, Hao Y, Xu J, Thun MJ. Cancer statistics, 2009. CA Cancer J Clin 2009;59:225–49.
2. Niciforovic A, Djordjevic J, Adzic M, Vucic V, Mitrasinovic PM, Radojcic MB. Experimental and systems biology studies of the molecular basis for the radioresistance of prostate carcinoma cells. Ann Biomed Eng 2008;36:831–8.
3. Buron C, Le Vu B, Cosset JM, et al. Brachytherapy versus prostatectomy in localized prostate cancer: results of a French multicenter prospective medico-economic study. Int J Radiat Oncol Biol Phys 2007;67:812–22.
4. van Tol-Geerdink JJ, Stalmeier PF, Pasker-de Jong PC, et al. Systematic review of the effect of radiation dose on tumor control and morbidity in the treatment of prostate cancer by 3D-CRT. Int J Radiat Oncol Biol Phys 2006;64:534–43.
5. Planchon S, Pink J, Tagliarino C, Bornmann W, Varnes M, Boothman D. β-Lapachone-induced apoptosis in human prostate cancer cells: involvement of NQO1/xip3. Exp Cell Res 2001;267:95–106.
6. Bentle MS, Reinicke KE, Bey EA, Spitz DR, Boothman DA. Calcium-dependent modulation of poly(ADP-ribose) polymerase-1 alters cellular metabolism and DNA repair. J Biol Chem 2006;281:33684–96.
7. Bentle MS, Reinicke KE, Dong Y, Bey EA, Boothman DA. Nonhomologous end joining is essential for cellular resistance to the novel antitumor agent, β-lapachone. Cancer Res 2007;67:6936–45.
8. Tagliarino C, Pink JJ, Dubyak GR, Nieminen AL, Boothman DA. Calcium is a key signaling molecule in β-lapachone-mediated cell death. J Biol Chem 2001;276:19150–9.
9. Tagliarino C, Pink J, Reinicke K, Simmers S, Wuerzberger-Davis S, Boothman D. Mu-calpain activation in β-lapachone-mediated apoptosis. Cancer Biol Ther 2003;2:141–52.
10. Bentle M, Bey E, Dong Y, Reinicke K, Boothman D. New tricks for old drugs: the anticarcinogenic potential of DNA repair inhibitors. J Mol Histol 2006;37:203–18.
11. Reinicke K, Bey E, Bentle M, et al. Development of β-lapachone prodrugs for therapy against human cancer cells with elevated NAD(P)H: quinone oxidoreductase 1 levels. Clin Cancer Res 2005;11:3055–64.
12. Bey EA, Wuerzberger-Davis SM, Pink JJ, et al. Mornings with Art, lessons learned: feedback regulation, restriction threshold biology, and redundancy govern molecular stress responses. J Cell Physiol 2006;209:604–10.
13. Drew Y, Plummer R. PARP inhibitors in cancer therapy: two modes of attack on the cancer cell widening the clinical applications. Drug Resist Updat 2009;12:153–6.
14. Peralta-Leal A, Rodriguez MI, Oliver FJ. Poly(ADP-ribose)polymerase-1 (PARP-1) in carcinogenesis: potential role of PARP inhibitors in cancer treatment. Clin Transl Oncol 2008;10:318–23.
15. Drew Y, Plummer R. The emerging potential of poly(ADP-ribose) polymerase inhibitors in the treatment of breast cancer. Curr Opin Obstet Gynecol ;22:67–71.
16. Farmer H, McCabe N, Lord CJ, et al. Targeting the DNA repair defect in BRCA mutant cells as a therapeutic strategy. Nature 2005;434:917–21.
17. Turner NC, Lord CJ, Iorns E, et al. A synthetic lethal siRNA screen identifying genes mediating sensitivity to a PARP inhibitor. EMBO J 2008;27:1368–77.
18. Noël G, Giocanti N, Fernet M, Mégnin-Chanet F, Favaudon V. Poly (ADP-ribose) polymerase (PARP-1) is not involved in DNA double-strand break recovery. BMC Cell Biol 2003;4:7.
19. Hegde ML, Hazra TK, Mitra S. Early steps in the DNA base excision/single-strand interruption repair pathway in mammalian cells. Cell Res 2008;18:27–47.
20. Kim MY, Zhang T, Kraus WL. Poly(ADP-ribosyl)ation by PARP-1: "PAR-laying" NAD^+ into a nuclear signal. Genes Dev 2005;19:1951–67.
21. Bey EA, Bentle MS, Reinicke KE, et al. An NQO1- and PARP-1-mediated cell death pathway induced in non-small-cell lung cancer cells by β-lapachone. Proc Natl Acad Sci U S A 2007;104:11832–7.
22. Boothman DA, Schlegel R, Pardee AB. Anticarcinogenic potential of DNA-repair modulators. Mutat Res 1988;202:393–411.
23. Boothman D, Pardee A. Inhibition of radiation-induced neoplastic transformation by β-lapachone. Proc Natl Acad Sci U S A 1989;86:4963–7.
24. Hermisson M, Wagenknecht B, Wolburg H, Glaser T, Dichgans J, Weller M. Sensitization to CD95 ligand-induced apoptosis in human glioma cells by hyperthermia involves enhanced cytochrome *c* release. Oncogene 2000;19:2338–45.
25. Pink JJ, Planchon SM, Tagliarino C, Varnes ME, Siegel D, Boothman DA. NAD(P)H:quinone oxidoreductase activity is the principal determinant of β-lapachone cytotoxicity. J Biol Chem 2000;275:5416–24.
26. Lee YJ, Galoforo SS, Berns CM, et al. Glucose deprivation-induced cytotoxicity and alterations in mitogen-activated protein kinase activation are mediated by oxidative stress in multidrug-resistant human breast carcinoma cells. J Biol Chem 1998;273:5294–9.
27. Lowry OH, Rosebrough NJ, Farr AL, Randall RJ. Protein measurement with the Folin phenol reagent. J Biol Chem 1951;193:265–75.
28. Lee JJ, Kong M, Ayers GD, Lotan R. Interaction index and different methods for determining drug interaction in combination therapy. J Biopharm Stat 2007;17:461–80.
29. Machado SG, Robinson GA. A direct, general approach based on isobolograms for assessing the joint action of drugs in pre-clinical experiments. Stat Med 1994;13:2289–309.
30. Min W, Wang ZQ. Poly(ADP-ribose) glycohydrolase (PARG) and its therapeutic potential. Front Biosci 2009;14:1619–26.
31. Boothman DA, Greer S, Pardee AB. Potentiation of halogenated pyrimidine radiosensitizers in human carcinoma cells by β-lapachone (3,4-dihydro-2,2-dimethyl-2*H*-naphtho[1,2-*b*]pyran-5,6-dione), a novel DNA repair inhibitor. Cancer Res 1987;47:5361–6.
32. Wuerzberger SM, Pink JJ, Planchon SM, Byers KL, Bornmann WG, Boothman DA. Induction of apoptosis in MCF-7: WS8 breast cancer cells by β-lapachone. Cancer Res 1998;58:1876–85.
33. Gerweck LE, Vijayappa S, Kurimasa A, Ogawa K, Chen DJ. Tumor cell radiosensitivity is a major determinant of tumor response to radiation. Cancer Res 2006;66:8352–5.
34. Lo SS, Fakiris AJ, Chang EL, et al. Stereotactic body radiation therapy: a novel treatment modality. Nat Rev Clin Oncol 2010;7:44–54.
35. Martin A, Gaya A. Stereotactic body radiotherapy: a review. Clin Oncol (R Coll Radiol) 2010;22:157–72.
36. Friedland JL, Freeman DE, Masterson-McGary ME, Spellberg DM. Stereotactic body radiotherapy: an emerging treatment approach for localized prostate cancer. Technol Cancer Res Treat 2009;8:387–92.
37. King CR, Brooks JD, Gill H, Pawlicki T, Cotrutz C, Presti JC, Jr. Stereotactic body radiotherapy for localized prostate cancer: interim results of a prospective phase II clinical trial. Int J Radiat Oncol Biol Phys 2009;73:1043–8.
38. Calabrese CR, Almassy R, Barton S, et al. Anticancer chemosensitization and radiosensitization by the novel poly(ADP-ribose) polymerase-1 inhibitor AG14361. J Natl Cancer Inst 2004;96:56–67.
39. Sakamoto-Hojo ET, Balajee AS. Targeting poly(ADP) ribose polymerase I (PARP-1) and PARP-1 interacting proteins for cancer treatment. Anticancer Agents Med Chem 2008;8:402–16.
40. Greco WR, Park HS, Rustum YM. Application of a new approach for the quantitation of drug synergism to the combination of *cis*-diamminedichloroplatinum and 1-β-D-arabinofuranosylcytosine. Cancer Res 1990;50:5318–27.
41. Chou TC, Talalay P. Quantitative analysis of dose-effect relationships: the combined effects of multiple drugs or enzyme inhibitors. Adv Enzyme Regul 1984;22:27–55.
42. Suzuki M, Amano M, Choi J, et al. Synergistic effects of fradiation and β-lapachone in DU-145 human prostate cancer cells *in vitro*. Radiat Res 2006;165:525–31.
43. Dong Y, Chin SF, Blanco E, et al. Intratumoral delivery of β-lapachone via polymer implants for prostate cancer therapy. Clin Cancer Res 2009;15:131–9.
44. Blanco E, Bey EA, Khemtong C, et al. β-Lapachone micellar nanotherapeutics for non-small cell lung cancer therapy. Cancer Res 2010;70:3896–904.